

Ab Initio SCF Study of the Addition of the Methyl Radical to Vinyl Compounds

Takayuki Fueno*

Department of Chemistry, Faculty of Engineering Science, Osaka University, Toyonaka, Osaka 560, Japan

Mikiharu Kamachi

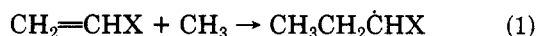
Department of Macromolecular Science, Faculty of Science, Osaka University, Toyonaka, Osaka 560, Japan. Received July 16, 1987

ABSTRACT: The addition reactions of the methyl radical to a few typical vinyl compounds $\text{CH}_2=\text{CHX}$, where $\text{X} = \text{OCH}_3$, CH_3 , H , COOH , CN , and $\text{C}\equiv\text{CH}$, have been dealt with by the UHF SCF procedure employing the conventional split-valence 3-21G basis functions. Geometries of both the adduct radicals and the transition states are fully optimized, to evaluate the reaction heats and the activation barrier heights. The absolute bimolecular rate constants for the case $\text{X} = \text{H}$, which are evaluated from the conventional transition state theory, are found to agree fairly well with the experimental gas-phase kinetic data. The activation barrier heights ΔE^\ddagger calculated for the various vinyl compounds have proved to be linearly related to the logarithms of Szwarc's "methyl reactivity" data for solution reactions. Characteristics of the transition states located are discussed on a quantitative basis.

Introduction

Addition reactions of alkyl radicals to olefins are not merely one of the most elementary types of organic reactions but are most fundamental to a proper understanding of the chemistry of vinyl monomers. Reactivity of vinyl compounds to radical species received considerable theoretical interest in the past, particularly in relation to their radical polymerizability.¹ To our surprise, however, virtually no attempt has ever been made to elucidate the energetics and reaction paths explicitly in regard to the potential energy surfaces. The pioneering work by Evans² is certainly illuminating to this issue but is admittedly too crude to be capable of furnishing as quantitative information as one could gain at the present age. It thus appears highly desirable to investigate the characteristics of radical reactions of vinyl monomers on a much less empirical ground than hitherto.

In this work, we have undertaken ab initio molecular orbital studies of the addition reactions of the methyl radical to a few vinyl compounds



where $\text{X} = \text{OCH}_3$, CH_3 , H , COOH , CN , and $\text{C}\equiv\text{CH}$. The formalism we adopt for this purpose is the unrestricted Hartree-Fock (UHF) SCF method. We will first work out full geometry optimizations of both the adduct radicals and the transition states, to evaluate the heats of the reaction and the activation barrier heights. The absolute rate constants for the case of $\text{X} = \text{H}$ in particular will then be predicted from the conventional transition state theory (TST) combined with the transition-state characteristics obtained here. Correlations of the activation barrier heights calculated for the various vinyl compounds with their experimental relative reactivity data will be examined. Finally, the effects of substituents on the structural characteristics of the transition states will be discussed in the light of the results obtained by the theoretical calculations.

Method of Calculation

SCF calculations were carried out using the Gaussian 70 program package³ available at the Institute for Molecular Science in Okazaki. The basis sets adopted for calculations are the conventional split-valence 3-21G functions.⁴

Geometries for the methyl radical and the reactant vinyl compounds were all optimized with the 3-21G basis sets. Full geometry optimizations were carried out for the adduct radicals with the aid of the UHF energy gradient technique. The minimum-energy paths for the addition reactions were traced by choosing the distance R between the methyl carbon atom and the β -carbon atom of the vinyl monomers as the principal reaction coordinate. The transition states (energy saddle points) for the addition reactions were located, to evaluate the activation barrier heights ΔE^\ddagger .

Normal-mode vibrational analyses were conducted only for the case where $\text{X} = \text{H}$. The force constant matrices required were constructed by numerical differentiations of the energy gradients involved.

Results

Reactants. The methyl radical was treated by the UHF SCF method. It was verified to be planar (D_{3h}) in form. The C-H bond length 1.072 Å obtained does not differ appreciably from the experimental distance 1.079 Å.⁵ The UHF SCF energy is -39.34261 hartree.

The vinyl compounds selected for examination in this work include methyl vinyl ether (OCH_3), propylene (CH_3), ethylene (H), acrylic acid (COOH), acrylonitrile (CN), and vinylacetylene ($\text{C}\equiv\text{CH}$). Their optimized geometries are illustrated in Figure 1, where the SCF energies obtained are also listed. It has been confirmed that methyl vinyl ether is the most stable in its s-cis (C_s symmetric) form with the methyl C-H bonds staggered to the $\text{C}^\alpha\text{-O}$ bond. Propylene is also C_s symmetric with one of the methyl C-H bonds eclipsed to the carbon-carbon double bond. The remaining vinyl compounds are all completely planar in structure.

Adduct Radicals. Geometries for the radicals formed by the addition of the methyl radical to the various vinyl monomers at the β -carbon have been optimized by the UHF SCF procedure. The optimized geometry for the case of methyl vinyl ether ($\text{X} = \text{OCH}_3$) as an example is illustrated in Figure 2. The olefinic carbon-carbon bond is elongated considerably as a result of the breaking-up of the π bonding. The α -carbon atom, which bears the OCH_3 group, loses its original sp^2 character. That is, the α -carbon moiety is pyramidalized in convex to the side away from the incoming CH_3 radical. In the case of $\text{X} = \text{OCH}_3$, the

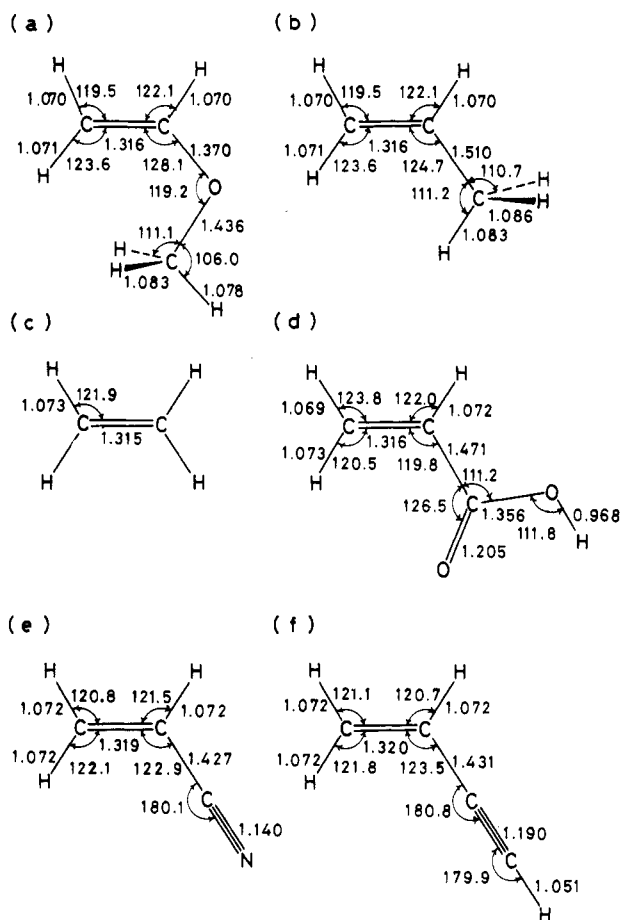


Figure 1. Optimized geometries of vinyl compounds (3-21G basis). The calculated total energies (hartree): (a) OCH_3 , -190.855 32; (b) CH_3 , -116.424 01; (c) H , -77.600 99; (d) COOH , -264.168 82; (e) CN , -168.820 40; (f) $\text{C}\equiv\text{CH}$, -152.856 22.

Table I
Structural Parameters Optimized and the Change in the Total Energy ΔE Calculated for the Adduct Radicals

X	$r(\text{C}^\alpha\text{C}^\beta)$, Å	$\phi(\text{H}^\alpha\text{C}^\alpha\text{C}^\beta\text{C}^\text{M})$, ^a deg	$\phi(\text{X}^\alpha\text{C}^\alpha\text{C}^\beta\text{C}^\text{M})$, ^a deg	ΔE , ^b kcal/mol
OCH_3	1.507	79.9	-59.5	-21.1 ₉
CH_3	1.508	79.0	-83.2	-23.9 ₆
H	1.509	80.9	-80.9	-24.4 ₀
COOH	1.498	83.0	-92.7	-29.9 ₁
CN	1.511	91.0	-85.6	-34.6 ₅
$\text{C}\equiv\text{CH}$	1.516	82.5	-92.6	-35.6 ₅

^a H^α and X^α denote respectively the hydrogen atom and the substituent atom which are attached to the α -carbon atom. C^M indicates the carbon atom of the attacking CH_3 radical. ^b Equation 2.

extent of this pyramidalization is particularly large, the dihedral angles $\phi(\text{O}^\alpha\text{C}^\alpha\text{C}^\beta\text{C}^\text{M})$ and $\phi(\text{H}^\alpha\text{C}^\alpha\text{C}^\beta\text{C}^\text{M})$ being -59.5° and 79.9° , respectively.

The carbon-carbon bond length $r(\text{C}^\alpha\text{C}^\beta)$ and the dihedral angles associated with the α -carbon atom, $\phi(\text{X}^\alpha\text{C}^\alpha\text{C}^\beta\text{C}^\text{M})$ and $\phi(\text{H}^\alpha\text{C}^\alpha\text{C}^\beta\text{C}^\text{M})$, as the structural parameters of importance, are compared among the various cases of substituents in Table I. Aside from the case of $\text{X} = \text{OCH}_3$, the pyramidalization of the C^α moiety is not appreciably large. These differences in the extent of pyramidalization may be related to the differences in the ESR α -H splitting constants $a(\text{H}^\alpha)$ observed for the propagating vinyl polymer ends. Thus, the $a(\text{H}^\alpha)$ values for the alkyl vinyl ether radical ends are noticeably smaller (16 G)⁶ than the values for the acrylic acid end (22 G)⁷ and the acrylonitrile end (20 G).⁷ The small $a(\text{H}^\alpha)$ values for

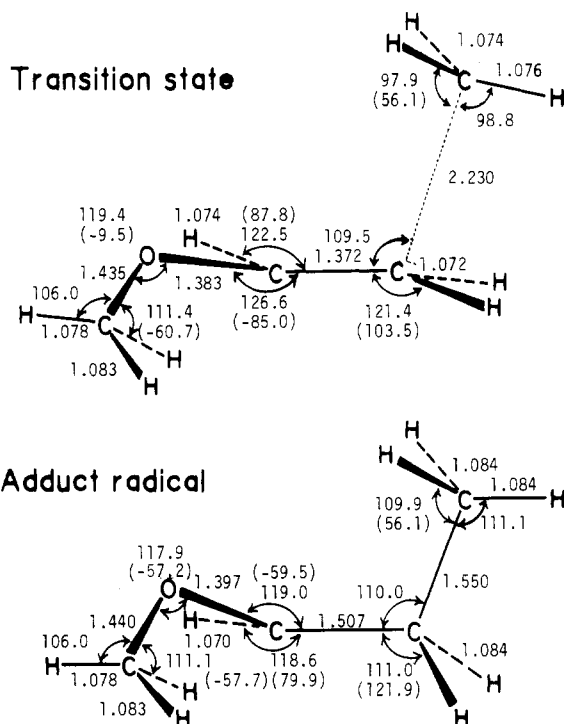


Figure 2. Optimized geometries of the product radical and the transition state for the addition of CH_3 to $\text{CH}(\text{OCH}_3)=\text{CH}_2$. Geometries in angstroms and degrees. () indicates the dihedral angle ϕ . For the ϕ 's associated with the α -hydrogen and oxygen atoms, see Table I. For the etheral bond, the angles $\phi(\text{COC}^\alpha\text{C}^\beta)$ are given. For each one of the methoxy, methyl, and β hydrogens, the values for $\phi(\text{HCO}^\alpha)$, $\phi(\text{C}^\alpha\text{C}^\beta\text{C}^\text{M}\text{H})$, and $\phi(\text{HC}^\beta\text{C}^\alpha\text{C}^\text{M})$ are shown, respectively.

the cases of vinyl ethers may be ascribable to the large pyramidalization and hence the increased s character of the α -C atom, as has been pointed out by Kamachi et al.⁶

Also given in Table I are the changes in the total SCF energy ΔE upon the methyl radical addition:

$$\Delta E = E(\text{CH}_3-\text{CH}_2\dot{\text{C}}\text{HX}) - E(\text{CH}_3) - E(\text{CH}_2=\text{CHX}) \quad (2)$$

The ΔE values calculated decrease from the top to the bottom of Table I, the addition of the CH_3 radical to vinylacetylene being the most exoergic.

The experimental heat of reaction is available for the case of ethylene ($\text{X} = \text{H}$), $\Delta H^\circ_{300} = -25.5$ kcal/mol.⁸ The energy change calculated in this work, $\Delta E = -24.4$ kcal/mol, is in reasonably good agreement with the experimental reaction heat, even though corrections for the vibrational zero-point energy and the heat capacity effects will be required on a more quantitative basis. The ΔE values calculated for the remaining cases are hoped to be accurate, probably to within 2 kcal/mol.

Transition States. The geometry of the transition state located for the case of $\text{X} = \text{OCH}_3$ is shown in Figure 2. The olefinic carbon-carbon bond length (1.372 Å) lies in between the lengths in the isolated monomer (1.316 Å) and the adduct radical (1.507 Å). The pyramidalizations of the two methylene moieties are not so large as in the adduct radical. The principal reaction coordinate, which has been defined as the distance between the methyl carbon atom and the monomer β -carbon atom, is $R^* = 2.230$ Å at the transition state. The methyl radical is seen to be only slightly pyramidalized at this stage of the addition reaction.

Transition state geometries for all the other cases were optimized likewise. Only the olefinic bond lengths $r(\text{C}^\alpha\text{C}^\beta)$

Table II
Optimal Structural Parameters for the Transition States,
the Calculated Activation Barrier Heights ΔE^* , and the
Experimental Methyl Reactivity Data $Z(\text{CH}_3)$

X	$r(\text{C}^\alpha\text{C}^\beta)$, Å	R^* , Å	ΔE^* , kcal/mol	$Z(\text{CH}_3)$
OCH_3	1.372	2.230	10.1 ₇	6
CH_3	1.374	2.265	7.3 ₃	22
H	1.375	2.270	6.7 ₂	34
COOH	1.367	2.328	3.6 ₅	1030 ^a
CN	1.377	2.370	1.6 ₅	1730
$\text{C}\equiv\text{CH}$	1.381	2.385	1.4 ₈	2260

^a The $Z(\text{CH}_3)$ value for methyl acrylate.^{11d}

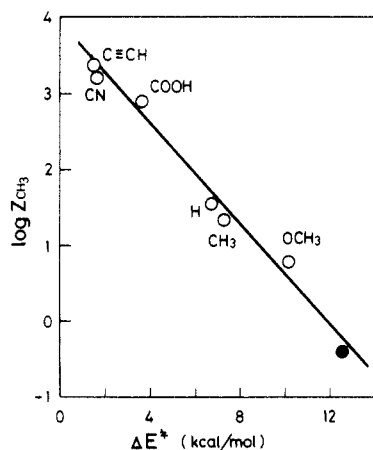


Figure 3. Plots of $\log Z(\text{CH}_3)$ against ΔE^* in the addition of CH_3 to $\text{CHX}=\text{CH}_2$: (●) benzene (4-31G basis, ref 12).

and the critical intermolecular distances R^* are given in Table II. The critical distance R^* is seen to increase as the exoergicity of reaction increases (from the top to the bottom).

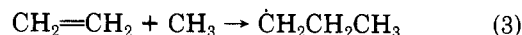
The activation barrier heights ΔE^* are the quantities of central importance in the present theoretical study. The values obtained for ΔE^* are given in Table II. The theoretical ΔE^* value of 6.7 kcal/mol obtained for the case of ethylene ($\text{X} = \text{H}$) agrees well with the experimental activation energy $E_a = 7.9$ kcal/mol⁹ as well as the value $\Delta E^* = 7.9$ kcal/mol calculated by the UHF-MINDO/3 method.¹⁰ Detailed comparison between theory and experiment will be made in the succeeding subsection.

As can be seen in Table II, the ΔE^* values decrease in increasing order of exoergicity (i.e., from the top to the bottom). Inspection of the R^* and ΔE^* values together indicates that the larger the R^* value, the smaller is the activation barrier height ΔE^* . The interrelations between R^* , ΔE , and ΔE^* will be discussed in more detail later.

The activation barrier heights ΔE^* calculated account for the variations in the "methyl reactivity" data $Z(\text{CH}_3)$, which have been reported by Szwarc et al.¹¹ The data are essentially the relative rate constants of various unsaturated compounds toward the methyl radical in isooctane. Of the vinyl compounds studied in this work, vinylacetylene takes on the smallest ΔE^* value and hence is predicted to be the most reactive, in harmony with the trend which the $Z(\text{CH}_3)$ values show.

Figure 3 shows plots of $\log Z(\text{CH}_3)$ against ΔE^* . The plotted points are seen to be fitted to a straight line. For the sake of comparison, the data $Z(\text{CH}_3) = 0.3^{11a}$ and $\Delta E^* = 12.3_8$ kcal/mol (4-31G calculation)¹² for benzene are included (filled circle) in Figure 3. Evidently, methyl vinyl ether is the least reactive of the vinyl monomers examined here but is more reactive than benzene, the ΔE^* value (10.1₇ kcal/mol) for the ether being significantly smaller than that (12.4 kcal/mol) for benzene.

Absolute Rate Constants. Cvetanović and Irwin⁹ carried out a kinetic study of the reaction



in the gas phase at temperatures of 300–500 K. The Arrhenius parameters for the rate constants are reported to be $A = 8.6 \times 10^{11} \text{ cm}^3 \text{ mol}^{-1} \text{ s}^{-1}$ and $E_a = 7.9$ kcal/mol in the temperature range studied.

We have undertaken to calculate the bimolecular rate constants for reaction 3 on the basis of the conventional transition state theory (TST),¹³ where the transmission coefficient is fixed at unity. Ab initio MO calculations of the transition state provide considerable reinforcement to the TST. Thus, we have the explicit TS geometry and the barrier height $\Delta E^* = 6.7_2$ kcal/mol, as has already been mentioned. Vibrational analysis of the transition state gives the normal-mode vibrational frequencies required for the calculation of the vibrational partition functions. The frequencies obtained are one, and only one, imaginary value of $473.3i \text{ cm}^{-1}$ plus 23 real frequencies, the smallest two of which are $\nu_1^* = 120.5$ (CH_3 twisting) and $\nu_2^* = 258.2$ ($\text{C}-\text{C}-\text{C}$ bending) cm^{-1} . The isolated reactants were also subjected to the normal-mode vibrational analysis. The vibrational zero-point energy correction was found to amount to $\Delta E_{\text{vib}}^* = 2.0_8$ kcal/mol. The theoretical activation energy is therefore $E_0 = 8.8_0$ kcal/mol. The TS model employing all of the 23 normal-mode vibrational frequencies as they are will here be referred to as model I.

Judging from the extremely small vibrational frequency (120.5 cm^{-1}) obtained, it seems likely that the attacking CH_3 group actually rotates nearly freely around the $\text{C}^\beta-\text{C}^{\text{M}}$ bond at the transition state. Thus, one may better assume an internal free rotation of the CH_3 group instead of its twisting vibration. The vibrational partition function with $\nu_1^* = 120.5 \text{ cm}^{-1}$ is now to be replaced by a one-dimensional rotation partition function¹³

$$Q_r^{(1)} = (8\pi^3 I^* k T)^{1/2} / \sigma^* h \quad (4)$$

where I^* denotes the one-dimensional moment of inertia and where σ^* is the symmetry number which is 3 in the present instance. Evaluation of I^* resulted in $I^* = 3.020 \text{ amu } \text{\AA}^2$. The vibrational zero-point correction reduces slightly to $\Delta E_{\text{vib}}^* = 1.9_1$ kcal/mol, to give the theoretical activation energy $E_0 = 8.6_3$ kcal/mol. The TS model, for which the one-dimensional free rotation of the CH_3 group and 22 vibrational normal modes are assumed, will be referred to as model II.

The rate constants were calculated according to both models I and II over the temperature range 300–500 K. In both cases, the symmetry numbers for ethylene and the methyl radical are 4 and 6, respectively. The calculated rate constants are compared with the experimental data in Figure 4. Both models give straight Arrhenius lines in the temperature region studied. The straight lines fitted to the Arrhenius equation $k = Ae^{-E_a/RT}$ are represented as follows:

model	A , $\text{cm}^3 \text{ mol}^{-1} \text{ s}^{-1}$	E_a , kcal/mol
I	6.16×10^{11}	8.51
II	6.38×10^{11}	8.06

Clearly, model II leads to the results in better agreement with experiments than does model I. The calculated rate constants are still too small by a factor of ca. 1.5. Yet, this much of disagreement will be permissible in view of the inherently approximate character of the theory as well as the method used in this work.

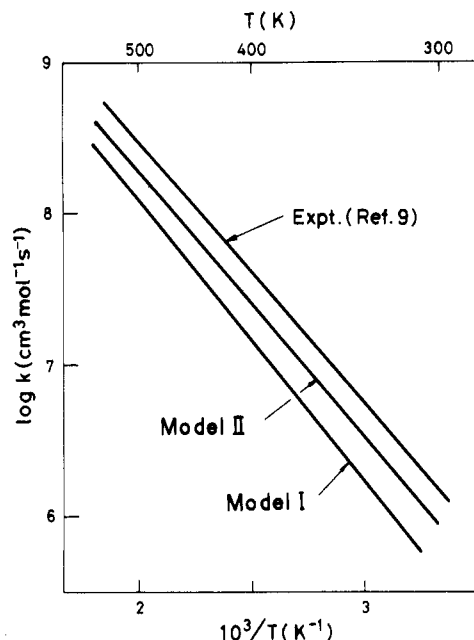


Figure 4. Rate constants for the reaction $\text{CH}_3 + \text{CH}_2=\text{CH}_2 \rightarrow \text{CH}_3\text{CH}_2\text{CH}_2$.

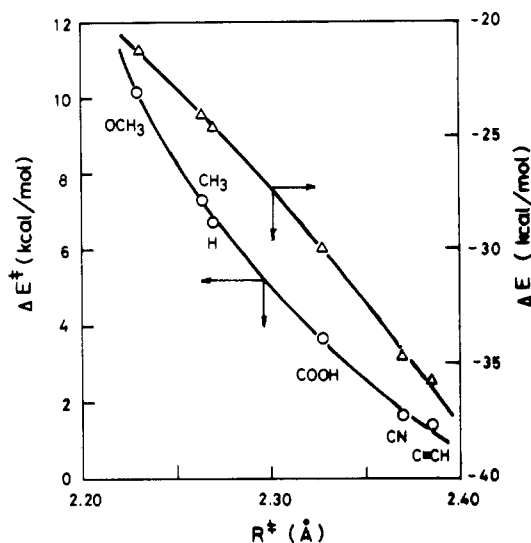


Figure 5. Plots of ΔE^* and ΔE against R^* for the additions of CH_3 toward $\text{CH}_2=\text{CHX}$.

Discussion

As has already been mentioned, the critical distance R^* at the transition state of the methyl radical addition is longer when the reaction is more exoergic. The trend noted is in line with Hammond's postulate:¹⁴ "In highly exothermic steps it will be expected that the transition states will resemble reactants closely..." The postulate can be paraphrased as implying that the greater the exothermicity for reactions of a given type, the more closely will their transition states resemble the reactant states. The relationship between the distance R^* and the exoergicity ΔE calculated is graphically shown in Figure 5.

Also shown in Figure 5 is the relationship between the activation barrier heights ΔE^* and the critical distance R^* . ΔE^* is seen to decrease monotonously with the increasing R^* . Thus, the barrier height ΔE^* tends to be lowered as the exoergicity of the reaction increases. This last statement is nothing but what is generally accepted for kinetic considerations of elementary reactions. A merit, if any, of the present treatment will lie in the success in quantitative demonstration of the relationship between ΔE^* and

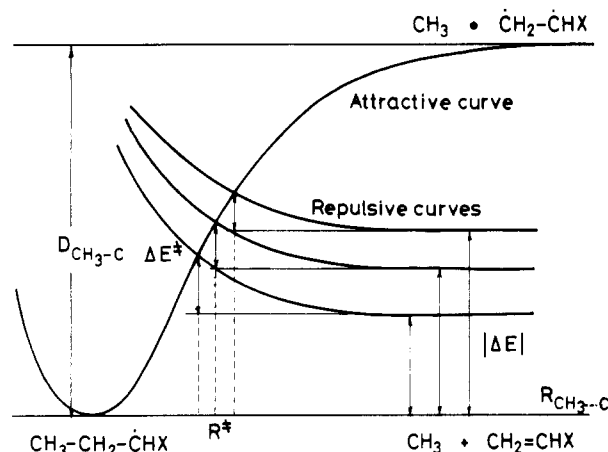


Figure 6. Diagrammatic representation of the potential energy profiles for the reactions $\text{CH}_3 + \text{CH}_2=\text{CHX} \rightarrow \text{CH}_3\text{CH}_2\text{CHX}$.

ΔE through the theoretically obtained R^* , which is a structural parameter of particular importance to the transition state.

Figure 6 presents diagrammatic illustrations of the effects of substituents on ΔE , ΔE^* , and R^* in the reactions of our present concern. The attractive curve is due to the bond formation between the methyl radical and the reaction center (β -carbon) of hypothetical vinyl substrates CH_2-CHX , in which the original C-C π bond has been broken. Since there is no direct interaction between the methyl group and the substituents X, the curve can be regarded as common to different vinyl substrates. The repulsive curves are considered to arise from the weakening of the vinyl bonding accompanying the progress of the addition reaction. The curves should all merge to the common level for $\text{CH}_3 + \dot{\text{C}}\text{H}_2\text{CHX}$ in the limit of complete breaking-up of the π bonding. At the initial state, however, the heights of these curves relative to the product radical should all differ from one another because of the differences in the loss of π conjugation on going from $\text{CH}_2=\text{CHX}$ to $\dot{\text{C}}\text{H}_2-\text{CHX}$. The different heats of reaction ΔE for different substituents X are the consequences of this situation. The crossing points between the attractive and repulsive curves correspond to the transition state. That the transition states appear at an earlier stage of the reaction in the cases in which $|\Delta E|$ are larger is self-explanatory from Figure 6.

It should be noted that our attractive-repulsive energetics considerations (Figure 6) are different from those that have originally been broached by Evans et al.² and used later by Buckley and Szwarc.^{11c} Both groups of authors assume that the repulsive curves result from the interaction of the methyl group with the π -electron cloud of the vinyl bond and that the curves are merged into a common level at the initial stage of reaction. The repulsive interaction of the type they assume should correspond to the exchange repulsion which is actually an adverse constituent of the attractive curve. The repulsion of this sort is overshadowed by the attractive charge-transfer interaction until the addition reaction has been completed, although it certainly dominates strongly in the region where R is less than the equilibrium bond length. In our view, the "repulsion" which is most relevant to the present consideration must be the one that arises from the local excitation of the π bonding and should eventually lead to the rupture of the bond. The importance of this effect in radical reactions in general has been stressed from the standpoint of the configuration expansion analysis.¹⁵ The repulsion will better be related to the triplet excitation or the localization energy of the substrate molecules. Only

by assuming different magnitudes of this energy inherent in different substrate molecules can the substituent effects on the heat of reaction be reconciled properly.

Finally, some comments on the symmetry factor involved in the rate constants seem to be in order. In calculating the bimolecular rate constant k for reaction 3, we have used the symmetry number $\sigma = 4$ for the isolated ethylene molecule. Because the transition state is planar symmetric (C_s), its symmetry number is $\sigma = 2$. Therefore, the rate constants calculated from the TST involve a substrate symmetry factor of $4/2 = 2$. This is tantamount to stating that the k values calculated are in reality the sum of those for the structurally equivalent two carbon atoms. In examining the relationships between $Z(\text{CH}_3)$ and ΔE^* (Figure 3), therefore, the $Z(\text{CH}_3)$ value for ethylene ($X = \text{H}$) should have been divided by 2. Likewise, the $Z(\text{CH}_3)$ for benzene would have to be divided by 6 in principle. Practically, however, such cautions have not led to any improvement of the $\log Z(\text{CH}_3) - \Delta E^*$ relationship. Discarding the symmetry factor in relating the experimental $Z(\text{CH}_3)$ to the theoretical ΔE^* will be permissible in view of the approximate nature of the calculation method used as well as the simplifications of the procedure adopted for the determinations of $Z(\text{CH}_3)$.

Acknowledgment. This work was supported in part by the Grants-in-Aid 60303001 and 61303003 from the Ministry of Education, Japan. The authors thank Professor S. Nozakura, Osaka University, for encouragements. They are also grateful to the Computer Center, Institute for Molecular Science, Okazaki, for an allocation of the CPU time.

Registry No. $\text{H}_2\text{C}=\text{CHOCH}_3$, 107-25-5; $\text{H}[\text{2C}=\text{CHCH}_3]$, 115-07-1; $\text{H}_2\text{C}=\text{CH}_2$, 74-85-1; $\text{H}_2\text{C}=\text{CHCO}_2\text{H}$, 79-10-7; $\text{H}_2\text{C}=\text{C}$ -

HCN , 107-13-1; $\text{H}_2\text{C}=\text{CHC}\equiv\text{CH}$, 689-97-4; CH_3^* , 2229-07-4.

References and Notes

- (1) For example: (a) Yonezawa, T.; Hayashi, K.; Nagata, C.; Okamura, S.; Fukui, K. *J. Polym. Sci.* **1954**, *14*, 312. (b) Hayashi, K.; Yonezawa, T.; Nagata, C.; Okamura, S.; Fukui, K. *J. Polym. Sci.* **1956**, *20*, 537. (c) Fueno, T.; Tsuruta, T.; Furukawa, J. *J. Polym. Sci.* **1959**, *40*, 487. (d) Kawabata, N.; Fueno, T.; Tsuruta, T.; Furukawa, J. *Bull. Chem. Soc.* **1963**, *36*, 1168.
- (2) Evans, M. G.; Gergely, J.; Seaman, E. C. *J. Polym. Sci.* **1948**, *3*, 866.
- (3) Hehre, W. J.; Lathan, W. A.; Newton, M. D.; Ditchfield, R.; Pople, J. A. QCPE Program No. 236, Indiana University, Bloomington, IN.
- (4) Binkley, J. S.; Pople, J. A.; Hehre, J. W. *J. Am. Chem. Soc.* **1980**, *102*, 939.
- (5) Herzberg, G. *Electronic Spectra and Electronic Structure of Polyatomic Molecules*; van Norstrand: New York, 1966.
- (6) Kamachi, M.; Tanaka, K.; Kuwae, Y. *J. Polym. Sci., Polym. Chem. Ed.* **1986**, *24*, 925.
- (7) Ranby, B.; Rebek, J. F. *ESR Spectroscopy in Polymer Research*; Springer-Verlag: Berlin, 1977.
- (8) Benson, S. *Thermodynamical Kinetics*, 2nd ed.; Wiley: New York, 1976.
- (9) Cvetanović, R. J.; Irwin, R. S. *J. Chem. Phys.* **1967**, *46*, 1694.
- (10) Dewar, M. J. S.; Olivella, S. *J. Am. Chem. Soc.* **1978**, *100*, 5290.
- (11) (a) Szwarc, M. *J. Polym. Sci.* **1955**, *16*, 367. (b) Leavitt, F.; Levy, M.; Szwarc, M.; Stannett, V. *J. Am. Chem. Soc.* **1955**, *77*, 5493. (c) Buckley, R. P.; Szwarc, M. *J. Am. Chem. Soc.* **1956**, *78*, 5696. (d) Herk, L.; Stefani, A.; Szwarc, M. *J. Am. Chem. Soc.* **1961**, *83*, 3008. (e) Szwarc, M.; Birks, J. H. *Theoretical Organic Chemistry*; Kekule Symposium; Butterworth: London, 1958; pp 271-278.
- (12) Fueno, T.; Yokota, S. *Chem. Lett.* **1987**, 1641.
- (13) Glasstone, S.; Laidler, K. J.; Eyring, H. *The Theory of Rate Processes*; McGraw-Hill: New York, 1941.
- (14) Hammond, G. S. *J. Am. Chem. Soc.* **1955**, *77*, 334.
- (15) Nagase, S.; Takatsuka, K.; Fueno, T. *J. Am. Chem. Soc.* **1976**, *98*, 3838. Nagase, S.; Fueno, T. *Bull. Chem. Soc. Jpn.* **1976**, *49*, 2929.

Nonterminated Chain Polymerization in a Convectionless Gas

H. Rabeony and H. Reiss*

University of California, Los Angeles, California 90024. Received June 29, 1987

ABSTRACT: We have investigated the steady-state distribution, with respect to degree of polymerization and location within the reaction chamber, of polymeric radicals produced by a gas-phase free radical chain reaction, under the following conditions. Initiating free radicals are produced, uniformly and at a constant rate, throughout a uniform monomer vapor in a reaction chamber in which the gases are free of convection, and the concentration of radicals is so low that recombinative termination is absent. The free radicals propagate into polymeric radicals which diffuse to the walls of the chamber where they are irreversibly adsorbed. The steady-state distribution results. For a cylindrical chamber with plane-parallel ends, we have been able to achieve an exact analytical result for the distribution even when both the propagation constant and diffusion coefficient depend on the degree of polymerization. Previously, an approximation to this distribution had been used to analyze data (obtained by using nucleation for detection) from styrene vapor, polymerized under the above conditions. We estimate the error in that approximation. The exact distribution is now available for future studies. Achievable degrees of polymerization depend on chamber size, and we illustrate the application of the theory with a simple example.

The Reaction System and Ultraslow Chemistry

It is possible to study¹ free radical, gas-phase chain polymerization under conditions where so few chains grow simultaneously that they cannot encounter one another so as to engage in bimolecular, recombinative termination. Indeed, in the case of styrene, where self-initiated thermal polymerization in the gas phase has been clearly demonstrated^{1,2} (at room temperature), only between 1 and 200 new chains appear to be initiated in a cubic centimeter

each second. More recent, not yet published, studies³ indicate that other vinyl monomers as well as dienes can be made to polymerize just as sparsely, if the gas is "doped" with an extremely small charge of peroxide initiator. Furthermore it appears possible to study ionic chains in the same manner.

Finally, there is the possibility that other kinds of initiators, e.g., metal carbonyls, as well as other kinds of polymers, e.g., inorganic polymers produced by a ring-